Chemical Engineering Journal 155 (2009) 508–513

Contents lists available at ScienceDirect

Chemical Engineering Journal

journal homepage: www.elsevier.com/locate/cej

K–V–Ca catalysts supported on porous alumina ceramic substrate for soot combustion: Preparation and characterization

Lina Sui*, Liyan Yu

College of Materials Science and Engineering, Qingdao University of Science and Technology, 53 ZhengZhou Road, Qingdao 266042, PR China

ARTICLE INFO

Article history:
Received 20 March 2009
Received in revised form 29 July 2009
Accepted 31 July 2009

Keywords:
Catalyst
Combustion
Catalytic activity

ABSTRACT

The KCl, KNO_3, $CaCl_2$, $Ca(NO_3)_2$, V–Ca and K–V–Ca catalysts supported on alumina ceramic substrates have been prepared. X-ray diffraction and thermogravimetry/differential scanning calorimetry were used to characterize the catalysts, and their catalytic activities were evaluated by a soot oxidation reaction using the temperature-programmed reaction system. The catalytic activity of KNO_3 is higher than KCl, and the catalytic activity of $Ca(NO_3)_2$ is as much as that of $CaCl_2$. The catalyst containing a higher KNO_3 content exhibits CO_2 adsorption, whereas higher $CaCl_2$ and $Ca(NO_3)_2$ content can restrain the adsorption of CO_2. The K–V–Ca catalyst with a molar ratio of 6:1:1 had the lowest soot onset combustion temperature. The melting and oxidation–reduction of KNO_3, oxygen content of catalyst surface, and formation of some eutectic phase may be the key factors in improving catalytic activity of catalysts.

1. Introduction

Diesel engines play a vital role in world economy, especially in transportation. Exhaust from traditional diesel engines using high-sulfur fuel contains high concentrations of respirable carbonaceous particles with absorbed organic compounds [1]. During the last few decades, concerns have grown on the negative effects that diesel particulate matter has on health. Because of this, particulate emissions were subjected to restrictions and various emission-reduction technologies were developed [2]. The combination of traps and oxidation catalysts appears to be the most plausible after-treatment technique to eliminate soot particles from diesel engines [3,4]. The science and technology of diesel particulate filters (DPF) have been reported [2,5]. In order to assure the regeneration of DPF, adopting catalytic oxidation is one of the effective methods. A potentially useful catalyst has to operate efficiently at low temperatures since the temperature of typical exhausts is 400 °C or below in light duty applications [6]. So the focus of present research in this field is to find a catalyst that could oxidize the soot at the exhaust temperature of 150–400 °C for modern diesel engine. Vanadate-based catalysts are effective for lowering the combustion onset temperature of diesel soot, such as Au–V-based catalyst [7], Cs–K–V catalysts [8], $CsVO_3$–MoO_3, Cs_2MoO_4–V_2O_5 [9–11], $Cs_4V_2O_7$ [12], and V_2O_5–Pt/SiO_2 catalysts [13]. It has been reported that the catalysts with addition of alkali metals are effective for lowering the combustion temperature of carbon [14–24], such as K–V–I and Cu–K–V–Cl/TiO_2 catalyst systems [25,26]. In the past decade, several investigations have been conducted to develop effective catalysts. Addition of some chloride salts ($FeCl_3$, NaCl and KCl) increases the catalytic activity, for example, $FeCl_3$–KCl/CuO can reduce the T_{max} of carbon oxidation from 780 to 500 °C [15]. KNO_3 supported on ZrO_2 have been studied for diesel soot combustion [27]. In this work, we report the synthesis of K–V–Ca catalysts supported on porous Al_2O_3 ceramics substrates. The catalytic oxidation activities for diesel soot were investigated in detail.

2. Experimental

2.1. Catalyst preparation

The chemicals used were analytical pure potassium chloride, potassium nitrate, ammonium metavanadate, calcium chloride and calcium nitrate. The theoretical compositions of the produced catalysts are shown in Table 1. The prepared catalysts were ground in a mortar for about 15 min to obtain the extremely fine mixed powders. Subsequently, 2 g of the fine powders was dissolved into 20 ml deionized water by grinding to achieve a paint-like mixture. The porous alumina ceramic substrates (dimension 20 mm × 15 mm × 1 mm) were impregnated with the paint-like mixture to get coating layer and then dried in an oven at 50 °C. After being dried, the mixture-coated substrates were calcined in a furnace at 600 °C for 3 h to obtain catalyst-coated substrates for catalytic oxidation measurement.

---

* Corresponding author. Tel.: +86 532 8402 2814; fax: +86 532 8402 2814.
E-mail address: linasui@126.com (L. Sui).

1385-8947/$ – see front matter © 2009 Elsevier B.V. All rights reserved.
doi:10.1016/j.cej.2009.07.053

Table 1
The theoretical compositions of the catalysts.

$KCl:NH_4VO_3:CaCl_2$ (molar ratio)	$KNO_3:NH_4VO_3:CaCl_2$ (molar ratio)	$KNO_3:NH_4VO_3:Ca(NO_3)_2$ (molar ratio)	$NH_4VO_3:Ca(NO_3)_2$ (molar ratio)
1:1:0.1	1:1:1	1:1:0.1	2:1
1:1:0.5	3:1:1	1:1:0.5	1:1
1:1:1	6:1:0.1	1:1:1	1:2
1:1:2	6:1:0.5	1:1:2	
	6:1:1		
	6:1:2		

2.2. Catalytic oxidation activity characterization

The temperature-programmed reaction (TPR) system was equipped with the nondisperse infrared (NDIR) CO and CO_2 online analyzer (Wuhan Cubic Optoelectronics Co. Ltd., China), and the data acquisition and recording units were used to evaluate the catalytic performances of the catalysts. Before TPR testing, the catalyst-coated substrate was fumed above the burning diesel directly to ensure that the obtained data is close to the real catalyst performance in the field. About 2 mg soot was loaded on the substrate. The soot onset ignition temperature (T_o), the peak temperature (T_p), and ΔT ($\Delta T = T_p - T_o$) were chosen for evaluating the catalytic activity of the catalyst. During the TPR test, the tube furnace was heated from room temperature to 500 °C at a heating rate of 10 °C/min with the CO_2-removed air fed into the furnace at a flow rate of 1 l/min.

2.3. Catalyst structure characterization

The crystalline phase of the catalyst materials was identified by powder X-ray diffraction (XRD) (Rigaku D/max-rA, Rigaku, Japan) equipped with a Cu Kα radiation source. Thermogravimetry/differential scanning calorimetry (TG–DSC) (STA 449C, Netzsch, Germany) was used to study the phase changes of the obtained catalysts. The thermal analyses were carried out at a heating rate of 10 °C/min.

2.4. Surface area determination

The specific surface areas of the catalysts were determined by the BET method in a NOVA-1000e surface area analyzer (American quantachrome).

3. Results and discussion

BET surface area data are presented in Table 2. It can be known that the NH_4VO_3–$Ca(NO_3)_2$ catalyst with a ratio of 1:1 has the lowest surface area. The surface area increases with the increase of the KNO_3 content. This demonstrates that the incorporation of KNO_3 can improve the disperse degree of the catalysts.

Fig. 1(A) shows the TPR curves of single-composition catalysts. As can be seen from Fig. 1(A), there are two peaks at 320 and 422 °C respectively on the TPR curve of KNO_3. The peak at 320 °C was suspected to attribute to the result of soot combustion. A new experimental procedure was then designed to identify the real soot onset combustion temperature. In this procedure, after finishing the first TPR run, we removed the samples from the furnace and coated them with diesel soot; we then immediately placed the samples into the hot furnace (about 300 °C) with CO_2-free air. The samples were cooled to room temperature in the furnace without contacting CO_2, and subsequently, the second TPR run started. The second TPR curve in Fig. 1(B) shows that the small peak disappeared. It is confirmed that the KNO_3 can adsorb CO_2, which also have been confirmed by previous study [28]. According to Fig. 1(A), the soot onset ignition temperatures are 412 °C and 392 °C for the pure KCl and KNO_3 catalysts. In addition, there is a peak at 442 °C on the TPR curve of KNO_3, while no peak is presented on the TPR curve of KCl. The soot onset ignition temperature of KNO_3 is lower than KCl, and the soot oxidation rate of KCl is slower than KNO_3. Carrascull et al. [27] have explained that KNO_3 plays an important role during soot oxidation. On the one hand, the molten potassium

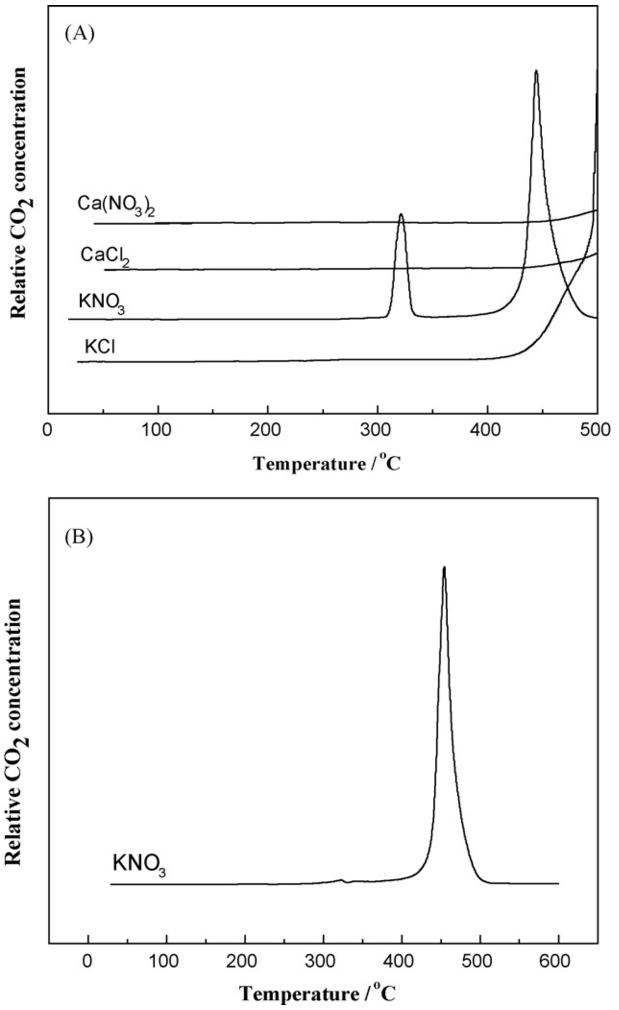

Fig. 1. TPR curves of simplex composition catalysts: (A) first TPR run and (B) second TPR run.

Table 2
BET surface areas of the catalysts.

Catalysts	BET surface area (m^2/g)
$KCl:NH_4VO_3:CaCl_2 = 1:1:0.5$	57.28
$KNO_3:NH_4VO_3:CaCl_2 = 6:1:1$	81.25
$NH_4VO_3:Ca(NO_3)_2 = 1:1$	53.42
$KNO_3:NH_4VO_3:Ca(NO_3)_2 = 1:1:0.1$	62.42
$KNO_3:NH_4VO_3:Ca(NO_3)_2 = 1:1:1$	68.67
$KNO_3:NH_4VO_3:Ca(NO_3)_2 = 6:1:1$	84.76

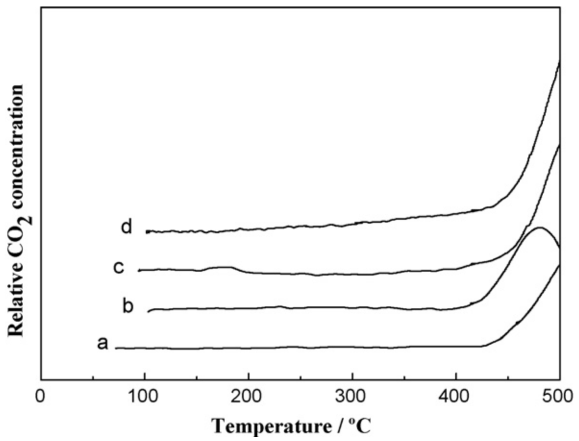

Fig. 2. TPR curves of KCl–NH_4VO_3–$CaCl_2$ catalysts: (a) KCl:NH_4VO_3:$CaCl_2$ = 1:1:0.1, (b) KCl:NH_4VO_3:$CaCl_2$ = 1:1:0.5, (c) KCl:NH_4VO_3:$CaCl_2$ = 1:1:1 and (d) KCl:NH_4VO_3:$CaCl_2$ = 1:1:2.

nitrate makes it possible to obtain good contact between the catalyst and diesel soot; on the other hand, the probable mechanisms are that one in which the nitrate is reduced to nitrite by the reaction with carbon and that the oxygen or the nitrogen oxide oxidize the nitrite again to nitrate.

$$2KNO_3 + C \rightarrow 2KNO_2 + CO_2$$

$$2KNO_2 + O_2 \rightarrow 2KNO_3$$

The soot combustion curves of pure $CaCl_2$ and $Ca(NO_3)_2$ catalysts are presented in Fig. 1(A). The soot onset ignition temperature of $CaCl_2$ at 430 °C is as much as that of $Ca(NO_3)_2$. In fact, $Ca(NO_3)_2$ starts to decompose at 500 °C, so CaO plays a key role during soot oxidation. The very low CO_2 concentrations on the TPR curves of $CaCl_2$ and CaO show that the catalytic activity of $CaCl_2$ and CaO is lower than KCl and KNO_3. Moreover, no low-temperature peaks on TPR curves confirm that $CaCl_2$ and CaO cannot adsorb CO_2.

The TPR curves of soot combustion in CO_2-removed airflow for KCl–NH_4VO_3–$CaCl_2$ catalysts supported on alumina substrates are plotted in Fig. 2. For the catalyst b, the soot onset ignition temperature is 398 °C, the peak temperature is 481 °C, and the ΔT is 83 °C. The other three catalysts present higher soot onset ignition temperature, and no peak temperature is presented on the TPR curves. So the catalyst b displays the lowest soot onset ignition temperature and the quickest soot oxidation rate among the four catalysts.

Fig. 3 presents the TPR curves of KNO_3–NH_4VO_3–$CaCl_2$catalysts. It can be seen from Fig. 3(A), the onset soot ignition temperature is 365 °C for catalyst a, there is a little increase at about 300 °C for catalysts b and f. However, three small peaks appear at 315, 347, and 333 °C for catalysts c, d, and e, respectively. The second TPR run curves are shown in Fig. 3(B). As can be seen from this figure, these little increase and small peaks disappear. So it can be concluded that the catalysts containing a certain amount of KNO_3 have a physical adsorption for CO_2. Both KNO_3 and $CaCl_2$ content have some effects on the amount of adsorbed CO_2. The higher the KNO_3 content of catalyst is, the larger the amount of adsorbed CO_2 is. However, the amount of adsorbed CO_2 decreased with the increase of $CaCl_2$ content. It can be seen clearly from Fig. 3 that the soot onset combustion temperatures and the peak temperatures for catalysts a, b, c, d, e and f are about 363, 354, 330, 328, 318, 330 °C and 470, 420, 427, 419, 406, 416 °C, respectively. So the ΔT is 107, 66, 97, 91, 88 and 86 °C, respectively. The catalyst e presents the lowest soot onset ignition temperature, and the catalyst b presents the quickest soot oxidation rate. To sum up, the catalytic activity of KNO_3:NH_4VO_3:$CaCl_2$ with a molar ratio of 1:1:1 is higher than KCl:NH_4VO_3:$CaCl_2$ with a molar ratio of 1:1:1.

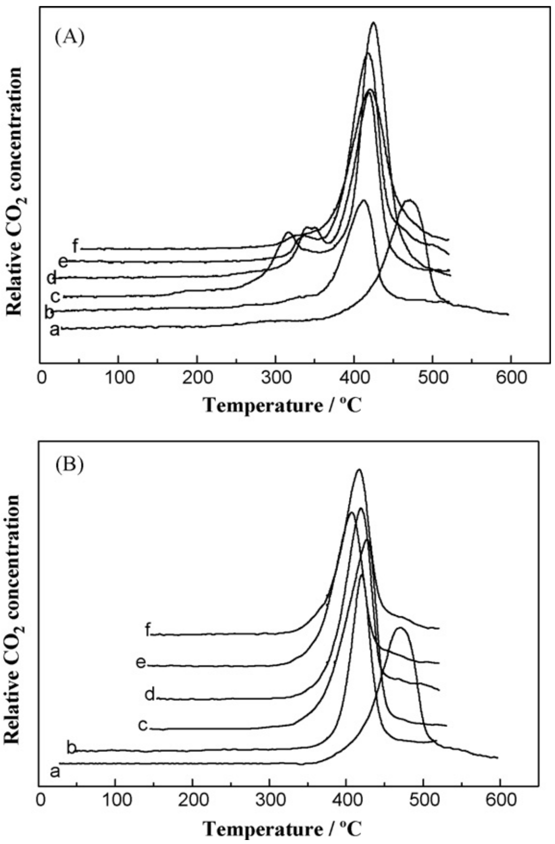

Fig. 3. TPR curves of KNO_3–NH_4VO_3–$CaCl_2$ catalysts: (A) first TPR run and (B) second TPR run. (a) KNO_3:NH_4VO_3:$CaCl_2$ = 1:1:1, (b) KNO_3:NH_4VO_3:$CaCl_2$ = 3:1:1, (c) KNO_3:NH_4VO_3:$CaCl_2$ = 6:1:0.1, (d) KNO_3:NH_4VO_3:$CaCl_2$ = 6:1:0.5, (e) KNO_3:NH_4VO_3:$CaCl_2$ = 6:1:1 and (f) KNO_3:NH_4VO_3:$CaCl_2$ = 6:1:2.

Fig. 4 presents the TPR curves of the KNO_3–NH_4VO_3–$Ca(NO_3)_2$ catalysts. There is a small increase at 300 °C for catalyst e and a small peak at 320 °C for catalyst f. The second TPR run curves shows that the small increase and small peak disappear. The catalysts a, b, c, d, e and f have an onset soot ignition temperature at 350, 350, 350, 367, 335 and 310 °C. The peak temperatures are 467, 463, 434, 470, 420 and 406 °C, and the ΔT are 117, 113, 84, 103, 85 and 96 °C for above six catalysts. The catalyst f presents the lowest soot onset ignition temperature and the catalyst e shows the quickest soot oxidation rate among the six catalysts. Compared catalyst c in Fig. 4 with the catalyst a in Fig. 3, it shows that the catalytic activity of KNO_3:NH_4VO_3:$Ca(NO_3)_2$ = 1:1:1 is better than that of KNO_3:NH_4VO_3:$CaCl_2$ = 1:1:1. The catalytic activity order is as follows: KNO_3:NH_4VO_3:$Ca(NO_3)_2$ = 1:1:1 > KNO_3:NH_4VO_3:$CaCl_2$ = 1:1:1 > KCl:NH_4VO_3:$CaCl_2$ = 1:1:1.

Fig. 5 is the TPR curves of NH_4VO_3–$Ca(NO_3)_2$. The soot onset ignition temperatures of the $Ca(NO_3)_2$–NH_4VO_3 catalysts are 398, 372 and 398 °C. The peak temperatures of catalysts a and b appear at 524 and 522 °C, whereas the peak temperature for the catalyst c appears at 550 °C. When the molar ratio of NH_4VO_3 and $Ca(NO_3)_2$ is 1:1, the soot onset ignition temperature is the lowest among the above three catalysts.

The X-ray diffraction patterns of the catalysts are presented in Fig. 6. The main crystalline phases of catalysts are listed in Table 3. The soot onset ignition temperature is 412 °C with the action of KCl, whereas it is 398 °C and it appears the peak at 481 °C in the cooperation between KCl and CaV_2O_6 for the KCl–NH_4VO_3–$CaCl_2$ catalyst with a molar ratio of 1:1:0.5. It illustrates fully that the

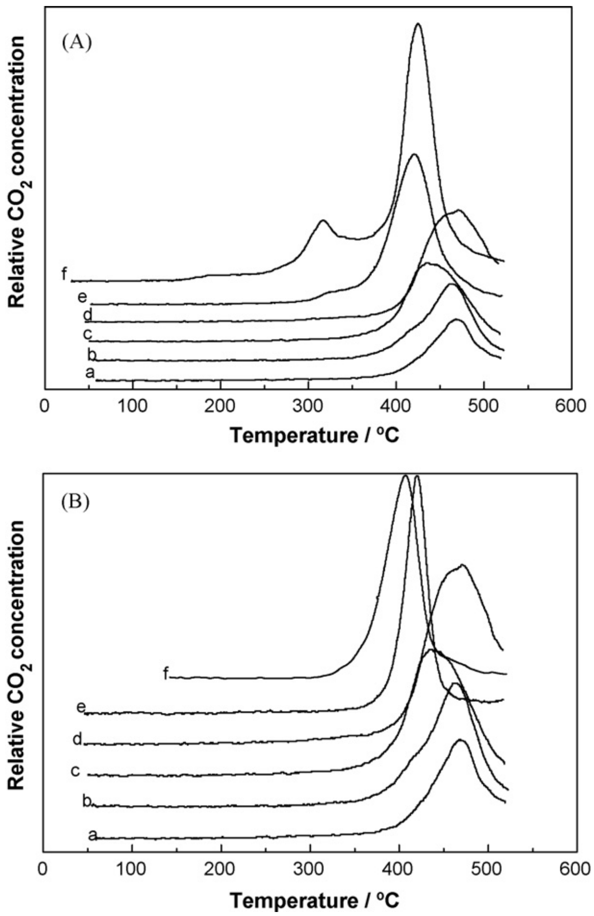

Fig. 4. TPR curves of KNO_3–NH_4VO_3–$Ca(NO_3)_2$ catalysts: (A) first TPR run and (B) second TPR run. (a) KNO_3:NH_4VO_3:$Ca(NO_3)_2$ = 1:1:0.1, (b) KNO_3:NH_4VO_3:$Ca(NO_3)_2$ = 1:1:0.5, (c) KNO_3:NH_4VO_3:$Ca(NO_3)_2$ = 1:1:1, (d) KNO_3:NH_4VO_3:$Ca(NO_3)_2$ = 1:1:2, (e) KNO_3:NH_4VO_3:$Ca(NO_3)_2$ = 3:1:1, (f) KNO_3:NH_4VO_3:$Ca(NO_3)_2$ = 6:1:1.

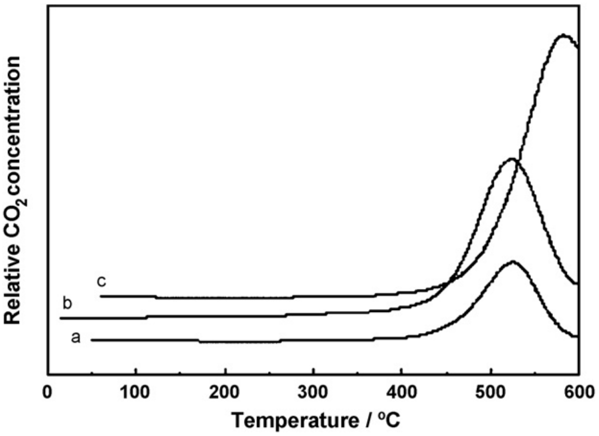

Fig. 5. TPR curves of NH_4VO_3–$Ca(NO_3)_2$ catalysts: (a) NH_4VO_3:$Ca(NO_3)_2$ = 2:1, (b) NH_4VO_3:$Ca(NO_3)_2$ = 1:1 and (c) NH_4VO_3:$Ca(NO_3)_2$ = 1:2.

Table 3
The main crystalline phases of catalysts.

Catalysts	Main crystalline phases
KCl:NH_4VO_3:$CaCl_2$ = 1:1:0.5	KCl, CaV_2O_6
KNO_3:NH_4VO_3:$CaCl_2$ = 6:1:1	KNO_3, CaV_2O_5, KCl
NH_4VO_3:$Ca(NO_3)_2$ = 1:1	$Ca_2V_2O_7$, CaV_2O_6, $Ca_{10}V_6O_{25}$
KNO_3:NH_4VO_3:$Ca(NO_3)_2$ = 1:1:0.1	KNO_3, KVO_3
KNO_3:NH_4VO_3:$Ca(NO_3)_2$ = 1:1:1	KNO_3, KVO_3, $Ca_3(VO_4)_2$
KNO_3:NH_4VO_3:$Ca(NO_3)_2$ = 6:1:1	KNO_3, $Ca_3(VO_4)_2$, $KCa_{10}V_7O_{28}$

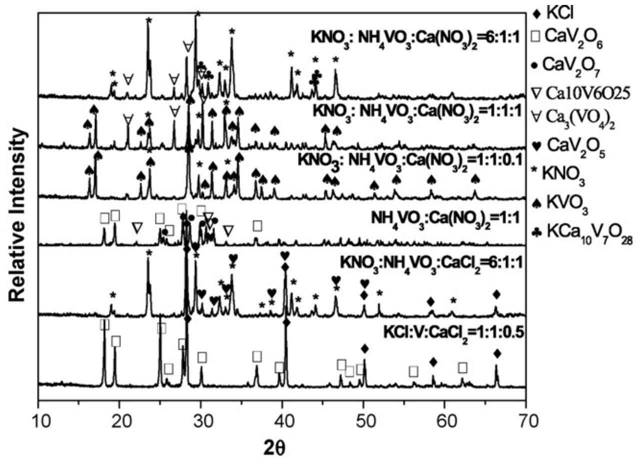

Fig. 6. XRD patterns of catalysts.

soot oxidation rate of the cooperation between KCl and CaV_2O_6 is more rapid than the pure KCl. It may be the presence of CaV_2O_6 increases the oxygen content on the surface of catalyst. In the cooperation of the crystalline phase $Ca_2V_2O_7$, CaV_2O_6 and $Ca_{10}V_6O_{25}$, the soot onset ignition temperature is 372 °C for the NH_4VO_3–Ca $(NO_3)_2$ catalyst with a molar ratio of 1:1, which is lower than pure $Ca(NO_3)_2$ and $CaCl_2$ catalysts. The soot onset ignition temperature is 350 °C with the action of KNO_3 and KVO_3, which is as much as that of KNO_3, KVO_3 and $Ca_3(VO_4)_2$. The soot oxygen rate ΔT is 84 °C at the presence of KNO_3, KVO_3 and $Ca_3(VO_4)_2$, which is more rapid than that of KNO_3 and KVO_3 with ΔT of 117 °C. At the presence of KNO_3, $Ca_3(VO_4)_2$ and $KCa_{10}V_7O_{28}$, the soot onset ignition temperature is lowered 40 °C than that of KNO_3, KVO_3, $Ca_3(VO_4)_2$. The high oxygen content of catalyst surface may be one of the key factors of improvement of catalytic activity. In addition, the high KNO_3 content is one main reason of lowering the soot onset ignition temperature. Though the KNO_3, $Ca_3(VO_4)_2$ and $KCa_{10}V_7O_{28}$ contain higher oxygen content than KNO_3, CaV_2O_5 and KCl, the catalytic activity of the two catalysts is almost the same. It can be seen from the XRD patterns that the KNO_3 peak is strong very much. So the catalytic oxidation of KNO_3 is very important. According to the previous publication [29], the onset ignition temperature is 369 °C for K–V catalyst with a ratio of 2:1 with the cooperation of the KCl, KVO_3 and $K_3V_5O_{14}$. It can be seen that K–V–Ca catalyst with a proper ratio can show better catalytic activity than K–V catalyst. Much work was devoted to K or V catalyst for the combustion of soot. KCl/CuO catalysts showed a start-up burning temperature at 500 °C [15]. Carrascull et al. [27] studied the KNO_3/ZrO_2 catalysts with a T_p at 395 °C. The catalytic combustion of soot was carried out in flowing $NO/O_2/He$ mixture (50 ml/min). T_p was 579 and 602 °C when the Cu–V/Al_2O_3 catalyst and soot were in tight contact and loose contact condition respectively [30]. It can be seen that K–V–Ca catalyst with a proper ratio can show better catalytic activity than above catalysts.

The DSC curves of catalysts are shown in Fig. 7. The catalyst a exhibits no evident variation below 500 °C. The catalyst b shows four endothermic effects at 129.8, 268.5, 314.9 and 359.3 °C. There are three peaks at 134.2, 306.6 and 474.3 °C on the DSC curve of catalyst c. There are three endothermic effects at 131.1, 324.2 and 435.7 °C on the DSC curve of catalyst d. Because catalysts b, c and d all contain KNO_3, the endothermic effects at 129.8/134.2/131.1 °C and 314.9/306.6/324.2 °C with no corresponding weigh loss should be attributed to the KNO_3 phase transformation and the melting of KNO_3. The variation of KNO_3 phase transformation temperature and melting temperature could be affected by other phases, so the DSC peaks deviated. The melting KNO_3 can enhance the contact

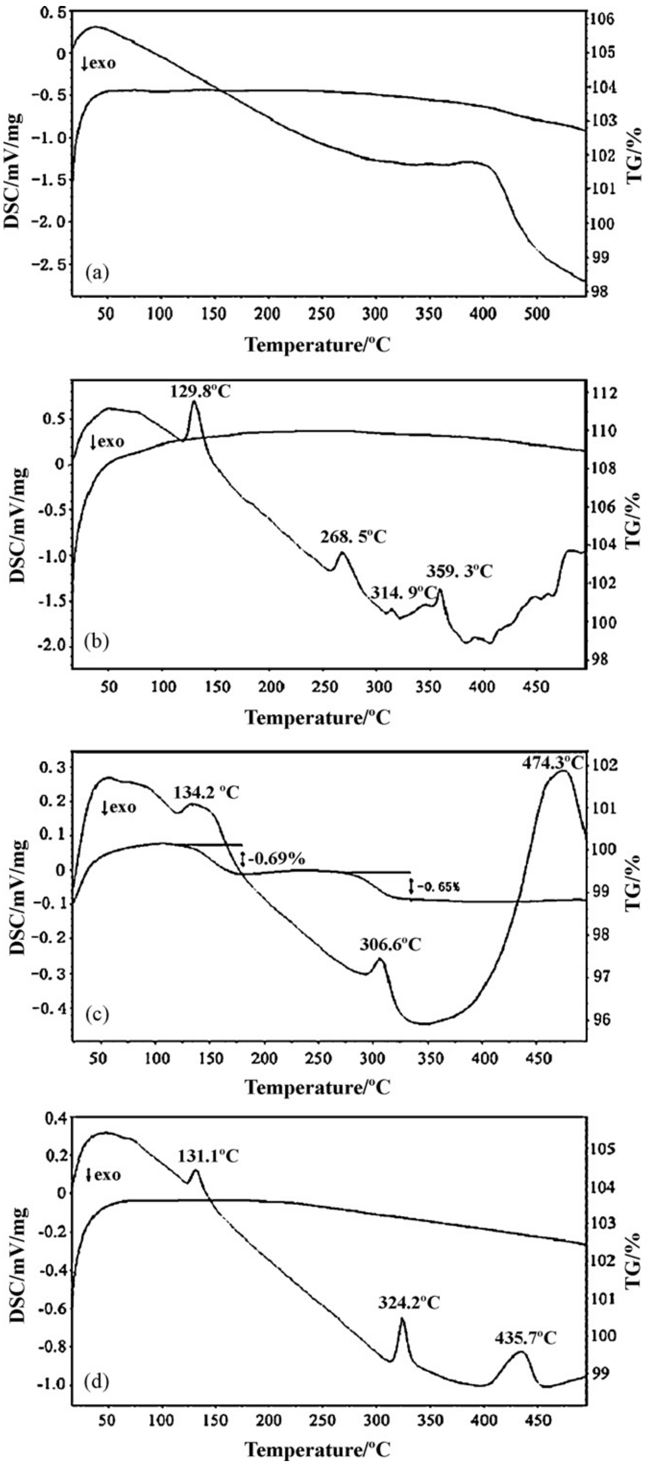

Fig. 7. The DSC curves of catalysts: (a) KCl:NH_4VO_3:$CaCl_2$ = 1:1:0.5, (b) KNO_3:NH_4VO_3:$CaCl_2$ = 6:1:1, (c) KNO_3:NH_4VO_3:$Ca(NO_3)_2$ = 1:1:0.1 and (d) KNO_3:NH_4VO_3:$Ca(NO_3)_2$ = 1:1:1.

between catalysts and soot, which leads to the improvement of the catalytic activity of catalysts. The peaks at 134.2 and 306.6 °C on the DSC curve of the catalyst b correspond to very little weight loss, which should be desorption of adsorbed CO_2 on the catalyst surface. The amount of adsorbed CO_2 is too little to be detected by TPR system. Because the KCl has no phase transformation and melting below 500 °C, the peaks at 268.5 and 359.3 °C attributed to the phase transformation or melting of CaV_2O_5. As the melting point of KVO_3 is 520 °C, either KVO_3 or $Ca_3(VO_4)_2$ has only a kind of XRD pattern, which means that both KVO_3 and $Ca_3(VO_4)_2$ have no phase transformation. For the peaks at 474.3 and 435.7 °C on the DSC curves, with no corresponding weight loss is likely attributed to the formation of a eutectic phase between KNO_3 and KVO_3 or KNO_3, KVO_3 and $Ca_3(VO_4)_2$. In addition, these peaks at 268.5 and 359.3 °C are also likely attributed to a eutectic phase that formed between the catalysts. If the two peaks at 268.5 and 359.3 °C are assigned to the melting of CaV_2O_5 or the formation of a eutectic phase, the surface mobility of the active phases is a key factor in the oxidation soot for catalyst b. The formation of liquid phases improves the catalyst/soot contact condition through a wetting process [19], which is likely the main reason for the lowering of the soot onset ignition temperature of catalyst b.

4. Conclusions

The K–V–Ca catalysts supported on α-porous alumina ceramic substrates have been produced and their compositions and catalytic activities for diesel soot oxidation were studied. The catalytic activity of KNO_3 is higher than KCl, and the catalytic activity of $Ca(NO_3)_2$ is as much as that of $CaCl_2$. The catalyst containing a higher KNO_3 content can promote the adsorption of CO_2, whereas the amount of adsorbed CO_2 decreases with the increase of $CaCl_2$ and $Ca(NO_3)_2$ content. According to the catalytic activity studies, the catalyst with KNO_3:NH_4VO_3:$CaCl_2$ and KNO_3:NH_4VO_3:$Ca(NO_3)_2$ molar ratio of 6:1:1 displayed the highest catalytic activity. The soot onset ignition temperature of crystalline phases should be in the order: $KCl + KNO_3 + CaV_2O_5 \approx KNO_3 + Ca_3(VO_4)_2 + KCa_{10}V_7O_{28} < KNO_3 + KVO_3 + Ca_3(VO_4)_2 \approx KNO_3 + KVO_3 < Ca_2V_2O_7 + CaV_2O_6 + Ca_{10}V_6O_{25} < KCl + CaV_2O_6$. According to the TG–DSC analysis, the melting of KNO_3 and CaV_2O_5 or the formation of eutectic phase is likely contributed to the highest catalytic activity of the catalyst with KNO_3:NH_4VO_3:$CaCl_2$ molar ratio of 6:1:1. To sum up, the melting and oxidation–reduction of KNO_3, oxygen content of catalyst surface and formation of some eutectic phases all can elevate catalytic activity of catalysts.

References

[1] T.W. Hesterberg, W.B. Bunn, R.O. McClellan, G.A. Hart, C.A. Lapin, Crit. Rev. Toxicol. 35 (2005) 379–411.
[2] B.A.A.L. van Setten, M. Makkee, J.A. Moulijn, Catal. Rev. 43 (2001) 489–564.
[3] I.C.L. Leocadio, S. Braun, M. Schmal, J. Catal. 223 (2004) 114–121.
[4] N.F. Galdeano, A.L. Carrascull, M.I. Ponzi, I.D. Lick, E.N. Ponzi, Thermochim. Acta 421 (2004) 117–121.
[5] V. Palma, M. D' Amore, P. Russo, A. D' Arco, P. Ciambelli, Combust. Sci. Technol. 174 (2002) 295–308.
[6] C.A. Querini, L.M. Cornaglia, M.A. Ulla, E.E. Miró, Appl. Catal. B 20 (1999) 165–177.
[7] J.V. Craenenbroeck, D. Andreeva, T. Tabakova, K.V. Werde, J. Mullens, F. Verpoort, J. Catal. 209 (2002) 515–527.
[8] C. Badini, G. Saracco, N. Russo, V. Specchia, Catal. Lett. 69 (2000) 207–215.
[9] S.J. Jelles, B.A.A.L. van Settern, M. Makkee, J.A. Moulijin, Appl. Catal. B 21 (1999) 35–49.
[10] S.J. Jelles, B.A.A.L. van Settern, M. Makkee, J.A. Moulijin, Stud. Surf. Sci. Catal. 116 (1998) 667–674.
[11] B.A.A.L. van Settern, R. van Dijk, S.J. Jelles, M. Makkee, J.A. Moulijin, Appl. Catal. B 21 (1999) 51–61.
[12] G. Saracco, C. Badini, N. Russo, V. Specchia, Appl. Catal. B 21 (1999) 233–242.
[13] S.T. Liu, A. Obuchi, J. Oi-Uchisawa, T. Nanba, S. Kushiyama, Appl. Catal. B 30 (2001) 259–265.
[14] E.E. Miró, F. Ravelli, M.A. Ulla, L.M. Cornaglia, C.A. Querini, Catal. Today 53 (1999) 631–638.
[15] S.B. Wang, B.S. Haynes, Catal. Commun. 4 (2003) 591–596.
[16] H.M. An, C. Kilroy, P.J. McGinn, Catal. Today 98 (2004) 423–429.
[17] S.B. Yuan, P. Mériaudeau, V. Perrichon, Appl. Catal. B 3 (1994) 319–333.
[18] A.L. Carrascull, M.I. Ponzi, E.N. Ponzi, Ind. Eng. Chem. Res. 42 (2003) 692–697.
[19] G. Neri, G. Rizzo, S. Galvagno, M.G. Musolino, A. Donato, R. Pietropaolo, Thermochim. Acta 381 (2002) 165–172.
[20] W.F. Shangguan, Y. Teraoka, S. Kagawa, Appl. Catal. B 12 (1997) 237–247.
[21] S. Xiao, K.W. Ma, X.Y. Tang, H. Shaw, R. Pfeffer, J.G. Stevens, Appl. Catal. B 32 (2001) 107–122.

[22] M.J. Illán-Gómez, S. Brandán, A. Linares-Solano, C. Salinas-Martínez de Lecea, Appl. Catal. B 25 (2000) 11–18.
[23] E.E. Miró, F. Ravelli, M.A. Ulla, L.M. Cornaglia, C.A. Querini, Stud. Surf. Sci. Catal. 130A (2000) 731–736.
[24] H.M. An, P.J. McGinn, Appl. Catal. B 62 (2006) 46–56.
[25] C. Badini, G. Saracco, V. Specchia, Catal. Lett. 55 (1998) 201–206.
[26] P. Ciambelli, V. Palma, P. Russo, S. Vaccaro, J. Mol. Catal. A: Chem. 204–205 (2003) 673–681.
[27] A. Carrascull, I.D. Lick, E.N. Ponzi, M.I. Ponzi, Catal. Commun. 4 (2003) 124–128.
[28] L.N. Sui, L.Y. Yu, Y.H. Zhang, Energy Fuel 20 (2006) 1392–1397.
[29] L.N. Sui, L.Y. Yu, Y.H. Zhang, J. Disper. Sci. Technol. 28 (2007) 285–289.
[30] J.P.A. Neeft, M. Makkee, J.A. Moulijn, Appl. Catal. B 8 (1996) 57–78.